Tight-Binding Calculations of the Optical Response of Optimally P-Doped Si Nanocrystals: A Model for Localized Surface Plasmon Resonance

Xiaodong Pi (皮孝东)[1,*] and Christophe Delerue[2,†]

[1]State Key Laboratory of Silicon Materials and Department of Materials Science and Engineering, Zhejiang University, Hangzhou 310027, China

[2]IEMN-Department ISEN, UMR CNRS 8520, Lille 59046, France

(Received 12 June 2013; published 25 October 2013)

We present tight-binding calculations in the random-phase approximation of the optical response of Silicon nanocrystals (Si NCs) ideally doped with large concentrations of phosphorus (P) atoms. A collective response of P-induced electrons is demonstrated, leading to localized surface plasmon resonance (LSPR) when a Si NC contains more than ≈ 10 P atoms. The LSPR energy varies not only with doping concentration but also with NC size due to size-dependent screening by valence electrons. The simple Drude-like behavior is recovered for NC size above 4 nm. Si NCs containing a large number of deep defects in place of hydrogenic impurities do not give rise to LSPR.

DOI: 10.1103/PhysRevLett.111.177402 PACS numbers: 78.67.Bf, 36.40.Gk, 71.45.−d, 73.22.−f

Nanocrystals (NCs) exhibiting localized surface plasmon resonance (LSPR) present remarkable optical properties, which are very attractive for a variety of applications such as biosensing [1] and photovoltaics [2]. Among plasmonic NCs, noble metal NCs are widely considered because of their strong LSPR in the visible range [3]. However, recent observations on the LSPR of semiconductor NCs that are either intrinsically doped with vacancies [4–6] or extrinsically doped with impurities [7–9] have received great attention because, in contrast to noble metal NCs, the LSPR of semiconductor NCs can be tuned by changing the doping level. In this Letter, we focus on NCs made of silicon (Si). This is not only because Si is a model semiconductor material, but also because Si-based plasmonics [10] is highly desired for the integration with microelectronics, optoelectronics, and photovoltaics. Similar to other semiconductor NCs [11,12], the doping of Si NCs is challenging, in particular given self-purification (dopant segregation to the NC surface) could occur [13]. In spite of these difficulties, the introduction of P and/or B impurities into Si NCs has been demonstrated [14–20]. There are even a few reports [21–24] showing high doping levels (>1 at %) compatible with plasmonic effects. However, it is only very recently that Rowe *et al.* [24] have demonstrated that heavily P-doped Si NCs synthesized via a nonthermal plasma technique [21] exhibit tunable LSPR in the energy range of 0.07–0.3 eV. In this work, and in those on other semiconductor NCs [4,5,9], the LSPR energy ω_{sp} (Mie resonance) for a spherical NC is believed to vary approximately as

$$\hbar\,\omega_{\mathrm{sp}} \approx \hbar\sqrt{\frac{ne^2}{\varepsilon_0 m_e(\varepsilon_b + 2\varepsilon_m)}}, \tag{1}$$

where n is the free-carrier concentration, e is the electronic charge, ε_0 is the free space permittivity, m_e is the free-carrier effective mass, ε_b and ε_m are the dielectric constants of the bulk semiconductor and medium, respectively. Equation (1) is obtained from the Drude theory in the limit where the width of the LSPR peak is small compared to $\hbar\omega_{\mathrm{sp}}$ and where $\varepsilon_b(\omega_{\mathrm{sp}})$ is close to its static value. It can be worked out from Eq. (1) that the LSPR energy could vary from 0.4 eV for $n = 1\%$ to 1.8 eV for $n = 20\%$ for $m_e^{\mathrm{Si}} = 0.3m_0$, $\varepsilon_b^{\mathrm{Si}} = 11.7$ (bulk Si values) and $\varepsilon_m = 1$ (Fig. 1), covering a technologically important range. But it is well known from theoretical [25–30] and experimental [16] works that a dopant in a semiconductor NC with a size smaller than the Bohr radius of the dopant does not behave like in the bulk, the carrier ionization energy is enhanced, the energy level is deeper, and the wave functions are more localized even if they spread over the entire NC volume [31]. Therefore the notion of free carriers is questionable in these systems and a deeper understanding of LSPR in doped semiconductor NCs is clearly needed. The simple Drude model gives an accurate description of the carrier dynamics in doped bulk Si [32]. But can we use it for Si NCs? What is the validity of Eq. (1)? What is the minimum number of active dopants and the minimum NC size needed to support LSPR? What is the effect of the quantum and dielectric confinements? Does the LSPR frequency depend on the NC size?

In the following, we address the above-mentioned important questions by studying the case of ideal P-doped Si NCs. Our calculations are based on self-consistent tight-binding (TB) theory in the random-phase approximation (RPA). We show that clear LSPR appears when the number of impurities in a Si NC is above ≈ 10. We obtain that the LSPR energy approximately varies as $\sqrt{n}$ like in Eq. (1) but also depends on the NC diameter, in particular due to a size-dependent screening [26,33,34]. The blueshift of the LSPR with decreasing size is described in terms of a two-component electron system, in analogy with the

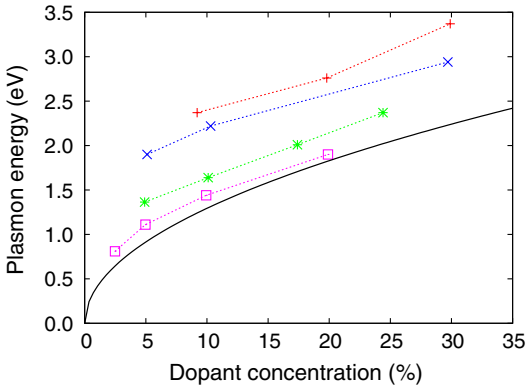

FIG. 1 (color online). Energy of the absorption peak with the highest intensity versus doping concentration for a Si NC. The diameter ($d = 2R$) of the NC is 1.8 (plus), 2.2 (cross), 3.2 (star), or 4.0 nm (square). The solid line represents the LSPR energy predicted by Eq. (1) with $m_e^{\mathrm{Si}} = 0.3m_0$, $\varepsilon_b^{\mathrm{Si}} = 11.7$ (bulk Si values) and $\varepsilon_m = 1$.

case of LSPRs in Ag NCs [35,36]. We show that Eq. (1) including bulk Si parameters accurately predicts the LSPR energy for NC diameters above ≈ 4 nm. It is demonstrated that Si NCs with deep defects like dangling bonds instead of P impurities do not show collective excitation.

Our goal in this Letter is to understand the physics of the formation of LSPR from electronic doping. Therefore we consider a model system in which Si NCs are hyperdoped up to $\approx 30\%$ without impurity segregation or lattice relaxation. We also assume that there is no dopant at the NC surface. All the impurities are in a configuration where they are electrically active in the bulk. We have performed TB calculations to obtain absorption spectra in a wide energy range for NCs containing up to 1200 Si atoms. The electronic states of energy E_n are written as $\psi_n = \sum_{i\beta} c_{n,i\beta}\phi_{i\beta}$, where $\phi_{i\beta}$ is the βth atomic orbital of the atom i at the position $\mathbf{R}_i$. The bare Hamiltonian matrix is expressed in a $sp^3d^5s^*$ basis as described in Ref. [37]. P atoms are placed at random substitutional positions excluding the atomic sites at the surface. We add to the bare TB Hamiltonian the Coulomb potential induced by a fixed charge $+e$ at each impurity nucleus (see Refs. [25,26]). We also add the Hartree potential coming from the extra electons. The self-consistent potential is obtained as described in Ref. [38]. The polarizability of a NC along a direction $\mathbf{u}$ at the energy E is given by $\alpha(E) = -e^2\sum_{i,j}\chi_{ij}^{\mathrm{RPA}}(\mathbf{R}_i \cdot \mathbf{u})(\mathbf{R}_j \cdot \mathbf{u})$, where χ^{RPA} is the self-consistent susceptibility matrix [39]. χ_{ij}^{RPA} represents the derivative of the electron population on the atom i with respect to the potential on the atom j. The matrix χ^{RPA} is given by $\chi^0\varepsilon^{-1}$, where $\varepsilon = I - V\chi^0$ is the dielectric matrix in RPA [40], I is the identity matrix, V is the matrix of the bare electron-electron interaction ($V_{ij} = e^2/|\mathbf{R}_i - \mathbf{R}_j|$) [26,41], and χ^0 is the independent-particle susceptibility matrix [40]

$$\chi_{ij}^0 = \sum_{n,n'} \frac{(f_n - f_{n'})(\sum_\beta c_{n,i\beta}c_{n',i\beta}^*)(\sum_\beta c_{n,j\beta}c_{n',j\beta}^*)}{E - (E_{n'} - E_n) + i\eta}, \qquad (2)$$

where f_n is the electronic population on the state n ($T = 300$ K). Details on the TB-RPA methodology can be found in Refs. [31,39,41]. Note that we have to include all possible transitions in Eq. (2) to obtain converged results, which require heavy computational resources even in TB. The polarizability $\alpha(E)$ scales as R^3, where R is the NC radius. The imaginary part of $\alpha(E)$ describes the absorbance at the energy E. The spectra presented below correspond to $\mathrm{Im}(\alpha(E)/R^3)$ with a broadening η of 0.1 eV.

The spectra obtained with the TB-RPA [Figs. 2 and 3(a)] exhibit very clear trends when we vary the number of P atoms. As this number is small (<10), the spectra are characterized by multiple peaks corresponding to the excitation of single electrons from the P-induced states to the conduction-band states. These peaks appear below the optical gap of the pristine Si NC. At an increasing number of P atoms, a broad peak emerges and becomes progressively prominent as the extra electrons brought by P atoms start responding collectively to the external field. At sufficiently high P concentration and NC size, the spectra are dominated by the LSPR. Interestingly, quite similar

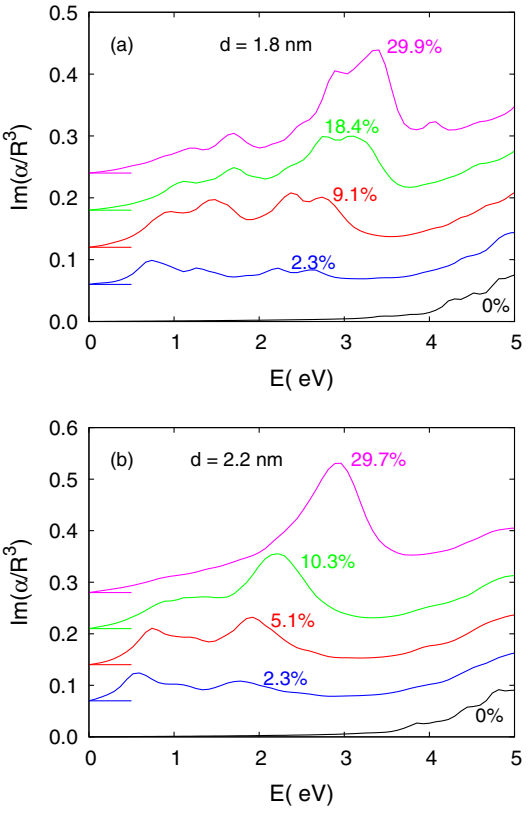

FIG. 2 (color online). Absorption spectra [$\mathrm{Im}(\alpha(E)/R^3)$] of (a) 1.8 nm Si NCs ($Si_{87}$) doped with 0, 2, 8, 16, and 26 P atoms. (b) Same for 2.0 nm Si NCs (Si_{175}) doped with 0, 4, 9, 18, and 52 P atoms. The corresponding doping levels are also indicated.

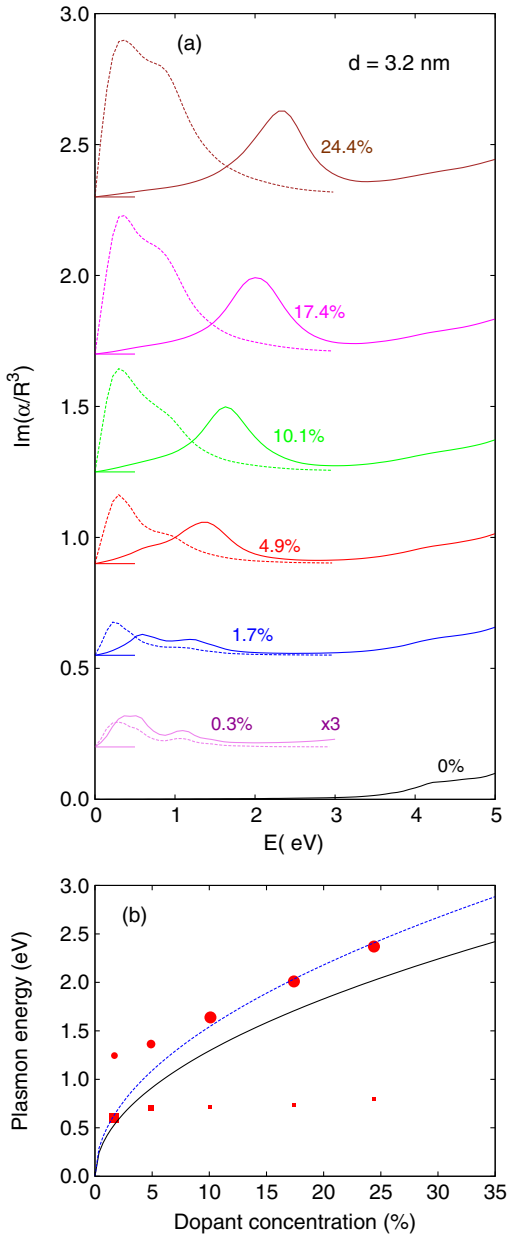

FIG. 3 (color online). (a) Absorption spectra [$\mathrm{Im}(\alpha(E)/R^3)$] of 3.2 nm Si NCs ($Si_{573}$) doped with 0, 2, 10, 28, 58, 100, and 140 P atoms. The corresponding doping levels are also indicated. The dotted lines show the spectra obtained by using the single-particle response instead of the self-consistent one, i.e., using $f_{\mathrm{lf}}^2\chi^0$ instead of χ^{RPA}. (b) Energy position of the high (circle) and low (square) energy Gaussian peak obtained from the decomposition of the absorption spectrum of a 3.2 nm Si NC containing ≥ 10 P atoms. The symbol size is proportional to the amplitude of the Gaussian peak. Solid line: $\hbar\omega_{\mathrm{sp}}$ predicted by Eq. (1) with $m_e^{\mathrm{Si}} = 0.3m_0$, $\varepsilon_b^{\mathrm{Si}} = 11.7$, and $\varepsilon_m = 1$. Dashed line: Same but with ε_b replaced by $\varepsilon^{\mathrm{Si}}(R) = 7.7$ [26].

behavior was predicted for Ag NCs when their size and therefore the number of free carriers were varied [42].

The interpretation of the broad peak as the result of LSPR is confirmed in Fig. 3(a). We compare the TB-RPA results with those obtained with the TB in the independent-particle approximation (IPA), i.e., replacing χ^{RPA} in the expression of $\alpha(E)$ with $f_{\mathrm{lf}}^2\chi^0$ where $f_{\mathrm{lf}} = 3/(\varepsilon_b + 2)$ is the local-field factor which describes the response of the dielectric sphere to the applied electric field [31]. In contrast to the self-consistent response of the RPA, the IPA only concerns a single-particle response. Therefore, absorption obtained with the IPA exclusively originates from single-electron excitations. Figure 3(a) shows that the two calculations only agree for very small numbers of P atoms (e.g., 2), but very quickly differ at higher doping levels. Above ≈ 10 P atoms per NC, we have found that each spectrum calculated in the TB-RPA [Fig. 3(a)] can be decomposed into two Gaussian peaks whose energy positions and amplitudes are given in Fig. 3(b). At increasing doping levels, the low-energy peak is centered at a constant position but its relative amplitude decreases whereas the position and the amplitude of the high-energy peak strongly increase. The prominent high-energy peak is not obtained in the TB-IPA. It indeed results from the collective response of electrons, i.e., the LSPR. The low-energy peak corresponds to single-electron excitations. Our results clearly demonstrate that single-electron and collective excitations coexist in doped Si NCs but collective ones dominate at high doping levels.

The energy $\hbar\omega_{\mathrm{sp}}$ of the LSPR is reported in Fig. 1 for NC sizes from 1.8 to 4.0 nm. It is clear that $\hbar\omega_{\mathrm{sp}}$ increases with the dopant concentration and scales as $\sqrt{n}$ (for $\gtrsim 10$ P atoms per NC), consistent with Eq. (1). The LSPR energy also depends on the NC size but tends at increasing NC size to approach the value predicted by Eq. (1). This behavior can be understood if we consider that $m_e(\varepsilon_b + 2\varepsilon_m)$ in Eq. (1) varies with the NC size. A large part of this variation can be explained by a reduced screening in semiconductor NCs [25,26,33]. This effect is not induced by the quantum confinement, i.e., by the opening of the gap, but is due to the breaking of polarizable bonds at the NC surface [31,34]. This leads to a size-dependent dielectric constant $\varepsilon^{\mathrm{Si}}(R)$ [26,33]. After the replacement of ε_b by $\varepsilon^{\mathrm{Si}}(R) = 1 + (\varepsilon_b^{\mathrm{Si}} - 1)/[1 + (0.92/R)^{1.18}]$ (see Ref. [26]), Eq. (1) fits quite well with the calculated LSPR energies for a NC size of 3.2 nm [Fig. 3(b)]. For smaller sizes, the size dependence of the dielectric constant does not fully explain the blueshift of the LSPR even if it predicts the correct trend. On the experimental side, Rowe *et al.* [24] interpreted their results on the LSPR of Si NCs with diameters above 5 nm by using Eq. (1). Our work totally justifies their approach.

In summary, the behavior of LSPR in P-doped Si NCs can be understood as follows. Under external excitation, the electrons brought by P atoms are polarized, forming a localized plasmon due to their strong intercoupling. But the field induced by this plasmon is screened instantaneously by the valence electrons since their corresponding plasmon energy is very high ($\approx$15 eV), justifying the presence of ε_b in the expression of the LSPR energy [Eq. (1)].

The shift of the LSPR to higher energy is explained by a less efficient screening by the valence electrons in small NCs. Therefore, impurity-doped NCs must be seen as two-component electron systems. Interestingly, the $1/R$ variation of the LSPR energy for Ag NCs was also explained by a size-dependent dielectric screening in a two-component electron system ($5s$ and $4p$ electrons) [35,36].

Figure 4 shows the absorption spectrum for a 3.2 nm Si NC containing 58 Si dangling bonds in place of P atoms. We have first removed 58 Si atoms and then passivated three of the four dangling bonds of each resulting vacancy by using hydrogen atoms. The dangling bonds give rise to deep energy levels in the gap. Compared to the same Si NC doped with 58 P atoms [Fig. 3(a)], the behavior is totally different. There are below-the-gap multiple peaks which result from the excitation of electrons between the bands and the deep energy levels. But the amplitudes of these peaks are small and there is no prominent peak typical of LSPR. The results obtained in TB-RPA or IPA are very similar (Fig. 4), indicating that collective effects are much less present. We conclude that the delocalization of the impurity-induced states in a NC is required to observe LSPR, as obtained with hydrogenic impurities such as P in Si NCs.

In conclusion, we have shown that Si NCs present LSPR when they are doped with more than ≈ 10 P atoms. In this condition, the LSPR energy of a Si NC varies with the carrier concentration according to the simple Drude model when the NC size is above ≈ 4 nm. For smaller Si NCs, the LSPR energy also depends on the NC size due to size-dependent screening. The decrease of the NC size actually mitigates the requirement of very high-level doping when one intends to increase the LSPR energy of a Si NC. Our work demonstrates that in the ideal situation LSPR with energies up to the visible range can be obtained in hyperdoped Si NCs. This should inspire experimentalists to confront the challenge of effectively hyperdoping Si NCs [12,24]. At this moment, it appears that hyperdoped Si NCs will be very likely produced in nonthermal plasma [21,24,43], in which thermodynamic equilibrium between Si NCs and background gas is absent. This may enable kinetically controlled doping of Si NCs up to levels well above the solubility limit. High dopant concentrations of 8.6 B at. % and 4.8 Al at. % have already been realized in Si films [44] and Si nanowires [45] via kinetics-controlled mechanisms, respectively. In addition, recent studies [46] also show that dopant concentrations of 9 As at. % and 11 P at. % can be obtained in Si NCs by ion beam synthesis [23]. It is hoped that the theoretical insights gained in this work will contribute to the development of Si-based plasmonics [10].

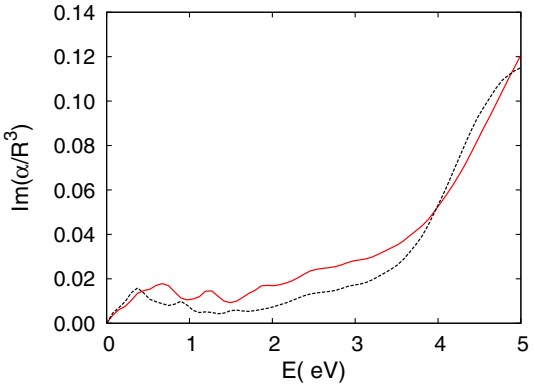

FIG. 4 (color online). Absorption spectrum [$\mathrm{Im}(\alpha(E)/R^3)$] of a 3.2 nm Si NC containing 58 Si dangling bonds (corresponding concentration of 10.1%) calculated in the TB-RPA (solid line) or TB-IPA (dashed line).

This work is supported by the National Basic Research Program of China (Grant No. 2013CB632101), the NSFC for excellent young researchers (Grant No. 61222404), and the Sino-French Xu Guangqi program.

*xdpi@zju.edu.cn
†christophe.delerue@isen.fr

[1] J. N. Anker, W. P. Hall, O. Lyandres, N. C. Shah, J. Zhao, and R. P. Van Duyne, Nat. Mater. **7**, 442 (2008).
[2] H. A. Atwater and A. Polman, Nat. Mater. **9**, 205 (2010).
[3] S. Link and M. A. El-Sayed, J. Phys. Chem. B **103**, 4212 (1999).
[4] J. M. Luther, P. K. Jain, T. Ewers, and A. P. Alivisatos, Nat. Mater. **10**, 361 (2011).
[5] F. Scotognella, G. Della Valle, A. R. Srimath Kandada, D. Dorfs, M. Zavelani-Rossi, M. Conforti, K. Miszta, A. Comin, K. Korobchevskaya, G. Lanzani, L. Manna, and F. Tassone, Nano Lett. **11**, 4711 (2011).
[6] Y. Zhao, H. Pan, Y. Lou, X. Qiu, J. Zhu, and C. Burda, J. Am. Chem. Soc. **131**, 4253 (2009).
[7] U. zum Felde, M. Haase, and H. Weller, J. Phys. Chem. B **104**, 9388 (2000).
[8] R. Buonsanti, A. Llordes, S. Aloni, B. A. Helms, and D. J. Milliron, Nano Lett. **11**, 4706 (2011).
[9] G. Garcia, R. Buonsanti, E. L. Runnerstrom, R. J. Mendelsberg, A. Llordes, A. Anders, T. J. Richardson, and D. J. Milliron, Nano Lett. **11**, 4415 (2011).
[10] R. J. Walters, R. V. A. van Loon, I. Brunets, J. Schmitz, and A. Polman, Nat. Mater. **9**, 21 (2010).
[11] S. C. Erwin, L. Zu, M. I. Haftel, A. L. Efros, T. A. Kennedy, and D. J. Norris, Nature (London) **436**, 91 (2005).
[12] D. J. Norris, A. L. Efros, and S. C. Erwin, Science **319**, 1776 (2008).
[13] T.-L. Chan, M. L. Tiago, E. Kaxiras, and J. R. Chelikowsky, Nano Lett. **8**, 596 (2008).
[14] M. Fujii, S. Hayashi, and K. Yamamoto, J. Appl. Phys. **83**, 7953 (1998).
[15] A. Mimura, M. Fujii, S. Hayashi, D. Kovalev, and F. Koch, Phys. Rev. B **62**, 12625 (2000).
[16] M. Fujii, A. Mimura, S. Hayashi, Y. Yamamoto, and K. Murakami, Phys. Rev. Lett. **89**, 206805 (2002).
[17] K. Sato, N. Fukata, and K. Hirakuri, Appl. Phys. Lett. **94**, 161902 (2009).
[18] M. Perego, C. Bonafos, and M. Fanciulli, Nanotechnology **21**, 025602 (2010).

[19] S. Kim, S. H. Hong, J. H. Park, D. Y. Shin, D. H. Shin, S.-H. Choi, and K. J. Kim, Nanotechnology **22**, 275205 (2011).
[20] H. Sugimoto, M. Fujii, K. Imakita, S. Hayashi, and K. Akamatsu, J. Phys. Chem. C **117**, 6807 (2013).
[21] X. D. Pi, R. Gresback, R. W. Liptak, S. A. Campbell, and U. Kortshagen, Appl. Phys. Lett. **92**, 123102 (2008).
[22] S. Gutsch, A. M. Hartel, D. Hiller, N. Zakharov, P. Werner, and M. Zacharias, Appl. Phys. Lett. **100**, 233115 (2012).
[23] R. Khelifi, D. Mathiot, R. Gupta, D. Muller, M. Roussel, and S. Duguay, Appl. Phys. Lett. **102**, 013116 (2013).
[24] D. J. Rowe, J. S. Jeong, K. A. Mkhoyan, and U. R. Kortshagen, Nano Lett. **13**, 1317 (2013).
[25] G. Allan, C. Delerue, M. Lannoo, and E. Martin, Phys. Rev. B **52**, 11 982 (1995).
[26] M. Lannoo, C. Delerue, and G. Allan, Phys. Rev. Lett. **74**, 3415 (1995).
[27] Z. Zhou, M. L. Steigerwald, R. A. Friesner, L. Brus, and M. S. Hybertsen, Phys. Rev. B **71**, 245308 (2005).
[28] F. Iori, E. Degoli, R. Magri, I. Marri, G. Cantele, D. Ninno, F. Trani, O. Pulci, and S. Ossicini, Phys. Rev. B **76**, 085302 (2007).
[29] X. D. Pi, X. B. Chen, and D. Yang, J. Phys. Chem. C **115**, 9838 (2011).
[30] X. B. Chen, X. D. Pi, and D. Yang, J. Phys. Chem. C **115**, 661 (2011).
[31] C. Delerue and M. Lannoo, *Nanostructures: Theory and Modeling* (Springer, New York, 2004).
[32] M. van Exter and D. Grischkowsky, Phys. Rev. B **41**, 12 140 (1990).
[33] L.-W. Wang and A. Zunger, Phys. Rev. Lett. **73**, 1039 (1994).
[34] C. Delerue, M. Lannoo, and G. Allan, Phys. Rev. B **68**, 115411 (2003).
[35] A. Liebsch, Phys. Rev. Lett. **71**, 145 (1993).
[36] F. Moresco, M. Rocca, T. Hildebrandt, and M. Henzler, Phys. Rev. Lett. **83**, 2238 (1999).
[37] Y. M. Niquet, D. Rideau, C. Tavernier, H. Jaouen, and X. Blase, Phys. Rev. B **79**, 245201 (2009).
[38] Y.-M. Niquet and C. Delerue, Phys. Rev. B **84**, 075478 (2011).
[39] J. J. H. Pijpers, M. T. W. Milder, C. Delerue, and M. Bonn, J. Phys. Chem. C **114**, 6318 (2010).
[40] L. Hedin and S. Lundqvist, in *Solid State Physics*, edited by H. Ehrenreich, F. Seitz, and D. Turnbull (Academic, New York, 1969), Vol. 23, p. 1.
[41] C. Delerue, M. Lannoo, and G. Allan, Phys. Rev. B **56**, 15 306 (1997).
[42] C. M. Aikens, S. Li, and G. C. Schatz, J. Phys. Chem. C **112**, 11 272 (2008).
[43] L. Mangolini and U. Kortshagen, Phys. Rev. E **79**, 026405 (2009).
[44] E. Bustarret, C. Marcenat, P. Achatz, J. Kacmarcik, F. Levy, A. Huxley, L. Ortega, E. Bourgeois, X. Blase, D. Debarre, and J. Boulmer, Nature (London) **444**, 465 (2006).
[45] O. Moutanabbir, D. Isheim, H. Blumtritt, S. Senz, E. Pippel, and D. N. Seidman, Nature (London) **496**, 78 (2013).
[46] D. Mathiot (private communication).